

Provided for non-commercial research and education use.
Not for reproduction, distribution or commercial use.



This article appeared in a journal published by Elsevier. The attached copy is furnished to the author for internal non-commercial research and education use, including for instruction at the authors institution and sharing with colleagues.

Other uses, including reproduction and distribution, or selling or licensing copies, or posting to personal, institutional or third party websites are prohibited.

In most cases authors are permitted to post their version of the article (e.g. in Word or Tex form) to their personal website or institutional repository. Authors requiring further information regarding Elsevier's archiving and manuscript policies are encouraged to visit:

<http://www.elsevier.com/copyright>



Photocapacitance measurements in irradiated a-Si:H based detectors

R. Schwarz^{a,*}, U. Mardolcar^a, Y. Vygranenko^b, M. Vieira^b, C. Casteleiro^c,
P. Stallinga^c, H. Gomes^c

^a Instituto Superior Técnico, Departamento de Física, 1049-001 Lisboa, Portugal

^b Instituto Superior de Engenharia de Lisboa, Departamento de Electrónica e Informática, 1959-007 Lisboa, Portugal

^c Universidade do Algarve, Faculty of Sciences and Technology, Campus de Gambelas, 8005-139 Faro, Portugal

Available online 31 January 2008

Abstract

Photocapacitance measurements were performed on amorphous silicon p–i–n detectors before and after particle irradiation with 1.5 MeV 4He^+ ions. The spatial resolution across a degraded spot is similar to the one obtained in photocurrent scans and is of the order of the diameter of the scanning laser beam. We monitored the transient capacitance after applying short laser pulses to deduce trap energies of 0.64 eV. Photocapacitance measurements as a function of the applied bias, the measurement frequency up to 1 MHz, and the wavelength of laser light are discussed. The reduction in photocapacitance signal and the shift of the cut-off frequency after ion bombardment are correlated with the change in transport properties.

© 2008 Published by Elsevier B.V.

PACS: 72.20.Jv; 72.40.+w; 73.61.Jc; 87.50.Gi

Keywords: Silicon; Sensors; Defects; Radiation

1. Introduction

When monitoring the degradation behaviour of elementary particle or X-ray detectors often the charge collection efficiency is taken as a figure of merit. Early work directed towards performance analysis of space solar cells used as power sources for satellites quotes the reduction of short-circuit current of such detectors after some exposure [1]. More detailed studies look for the changes in both the electron and hole transport properties, the creation mechanisms of defects, their energetic level and their density, internal electric field distributions, and recombination kinetics. A new way of measuring the density-of-states distribution in amorphous semiconductors was introduced through photocapacitance spectroscopy [2]. It is in some

sense similar to the well-known constant photocurrent method, CPM, and to thermal deflection spectroscopy [3].

Recently, several defect levels were identified by temperature-dependent spectral photocapacitance measurements in single films of ZnO [4] and CdTe [5]. Other authors applied this technique to complete amorphous silicon based p–i–n solar cells and described a combination of photocapacitance measurements and solar cell parameter measurements, combined with a computer model to show that under strong illumination the photocharge increases inside the solar cell and causes field collapse and thus a decline in solar cell efficiency [6]. A more theoretical treatment was given in Ref. [7], where the authors considered the photocapacitance C_{ph} to be a measure of the density of photogenerated carriers in the space charge region of a pin detector structure. It follows that both the electric field and the transport properties of photogenerated charges determine to the photocapacitance signal. In particular, the mobility and recombination lifetime of the minority carriers, which are generally holes, are important.

* Corresponding author. Tel.: +351 218419152; fax: +351 218419118.
E-mail address: rschwarz@fisica.ist.utl.pt (R. Schwarz).

2. Sample structure and measurement procedure

In most of the presented experiments we address the characteristics of photocurrent and of photocapacitance using a $1.1\ \mu\text{m}$ thick and $1.5\ \text{mm} \times 6.8\ \text{mm}$ large p–i–n detector sample (sample B-201-U) prepared at the University of Waterloo. A portion of the wire-bonded chip that includes pixels of different size is shown in Fig. 1. For comparison, other p–i–n detectors, prepared at the University of Stuttgart and the Hahn-Meitner-Institut in Berlin (samples HMI-2 and HMI-3), with a large range of i-layer thickness and pixel size, were also studied.

The detectors were exposed to a 1.5 MeV helium beam reaching a fluence of $1.5 \times 10^{15}\ \text{cm}^{-2}$ at the ITN accelerator in Lisbon. The effect of particle irradiation is easily discernable in Fig. 1. The detector (B-201-U) was irradiated at three locations, marked by the white dotted circles. The first degraded spot of about 1 mm diameter (particle beam size) is seen at the left side by the damage caused to the metal contacts.

Experimentally, there are different ways to measure C_{ph} . For time-resolved capacitance measurements we used lock-in detection of the out-of-phase current through the device. Typically, we applied a sinusoidal modulation signal of 100 mV at 16 kHz and HeNe laser light modulation at 63 Hz. A commercial capacitance bridge was used for the measurements as a function of bias voltage and modulation frequency (C – V – f plots).

3. Experimental results

We first studied the temporal behaviour of the photocapacitance signal in the ms range by applying HeNe laser pulses of 60 ms of duration and then monitoring the capacitance decay. Fig. 2 shows the result in sample HMI-3 which has an intermediate thickness of $2\ \mu\text{m}$. The illumination density was about $0.3\ \text{mW}/\text{cm}^2$ when using a neutral density filter of $\text{ND} = 1.7$. The increase is about 17 pF.

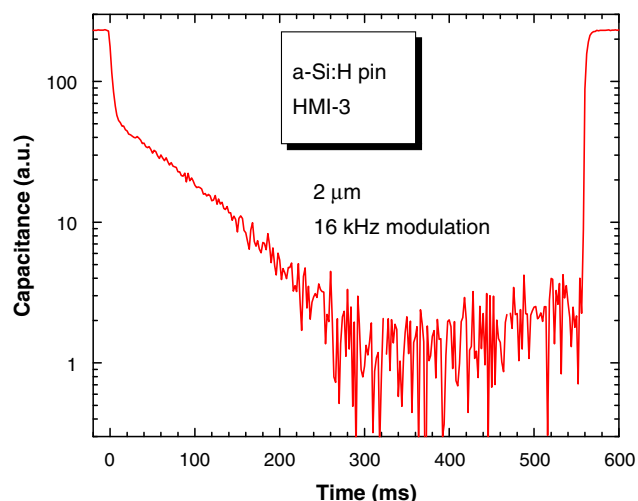


Fig. 2. Photocapacitance transients in the $2\ \mu\text{m}$ thick p–i–n detector HMI-3 under HeNe laser pulses of 60 ms duration. The semi-logarithmic representation of the photocapacitance decay after switching off the HeNe laser shows a characteristic decay time of 96 ms at room temperature.

After the light is turned off, the capacitance does not return immediately to its dark value, but shows an exponential decay as seen by the straight line in the semi-logarithmic plot.

The same test with the $5\ \mu\text{m}$ thick HMI-2 detector did not lead to conclusive results. The capacitance was much lower. One reason could have been that, at least for zero bias and for reverse bias operation, the capacitance change is too low for our set-up.

The remaining measurements are all done with the $1.1\ \mu\text{m}$ thick B-201-U detector sample that had a number of different pixel sizes. We employed at that stage the commercial capacitance bridge which has a much higher resolution, even though time-resolved measurements were not possible.

Fig. 3 shows a photocapacitance scan along the $6.8\ \text{mm}$ long and $1.6\ \text{mm}$ wide center pixel of the detector B-201-U

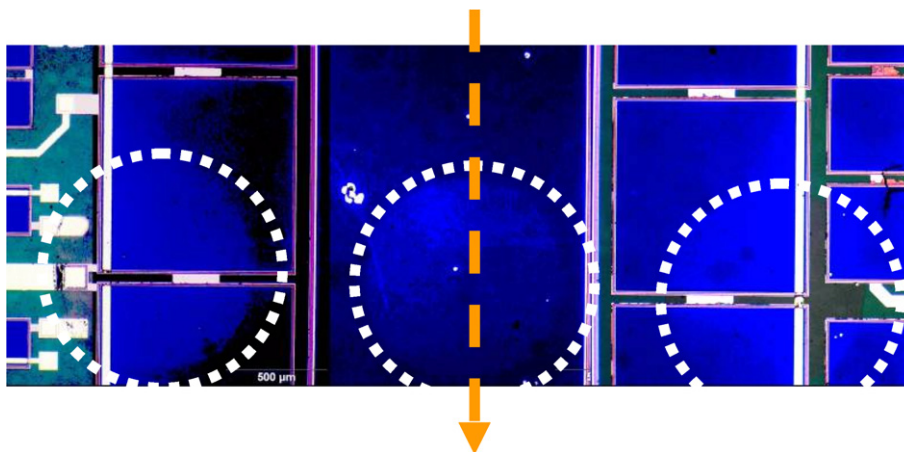


Fig. 1. Optical micrograph of the $1.1\ \mu\text{m}$ thick detector (B-202-U) irradiated at three locations, marked by the white dotted circles. The first spot on the left of about 1 mm diameter is easily seen by the damage caused to the metal contacts. The vertical arrow indicates the scan direction of the laser beam. The width of the squares is 1.6 mm.

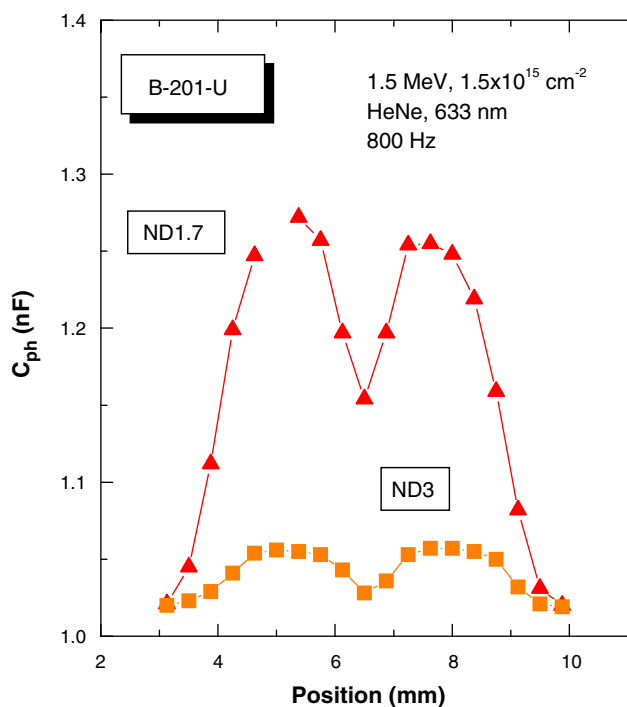


Fig. 3. Photocapacitance scan along the 6.8 mm long and 1.6 mm wide center pixel of the detector B-202-U of 1.1 μm thickness, irradiated by 1.5 MeV 4He^+ ions with accumulated fluence of $1.5 \times 10^{15} \text{ cm}^{-2}$. ND denotes the strength of the neutral density filters to attenuate the HeNe laser beam used for readout.

of 1.1 μm thickness, irradiated by 1.5 MeV 4He^+ ions with accumulated fluence of $1.5 \times 10^{15} \text{ cm}^{-2}$. ND denotes the strength of the neutral density filters to attenuate the HeNe laser beam used for readout. The central dip corresponds to the size of the helium beam. The beam shape is probably not Gaussian, since a mechanical aperture was used to limit the beam size. The optical micrograph in Fig. 1 hints even to an isotropic particle flux density across the beam.

Next we analysed the frequency dependence of the capacitance in dark (Fig. 4(a)) and under HeNe laser illumination for the three applied bias voltages, 0.5 V for forward bias, zero Volt, and -0.5 V for reverse bias condition. A strong photocapacitance signal is seen for low frequency (below 1 kHz) and for forward bias condition.

In Fig. 5 we show the voltage dependence of the photocapacitance taken at 1 kHz modulation frequency for the case of HeNe and HeCd illumination. The lower curve shows the result in dark. We made an attempt to present the data of Fig. 5(a) in a Mott plot (see Fig. 5(b)), and we can identify a linear region with the straight lines intersecting the x -axis at about 0.65 eV.

Finally, in Fig. 6 we studied the changes introduced by the He ion bombardment. The upper C - V - f curve is taken before irradiation. The photocapacitance signal is strongly reduced after bombardment, whereas the frequency dependence is similar over the total range of 100 Hz to 1 MHz. However, after subtracting the dark capacitance curve and after multiplying the degraded curve with a factor that allows easy comparison, we can see that the cut-off frequency actually dropped from about 3.5 kHz (defined by the 10% level of capacitance change) down to about 1.2 kHz.

4. Discussion

The characteristic decay time of 96 ms deduced from the data of Fig. 2 can be interpreted as a characteristic recombination time, or as a typical reemission time of carriers trapped at some energy E_{trap} . Assuming a phonon frequency of 10^{12} Hz we obtain a trap depth E_{trap} of 642 meV. The alternative interpretation of recombination lifetime is not probable if one compares the decay with photocurrent transients that show characteristic times in the μs range. The modulation frequency was chosen at 16 kHz in this case, indicating that the measurement was not dominated by an RC time constant.

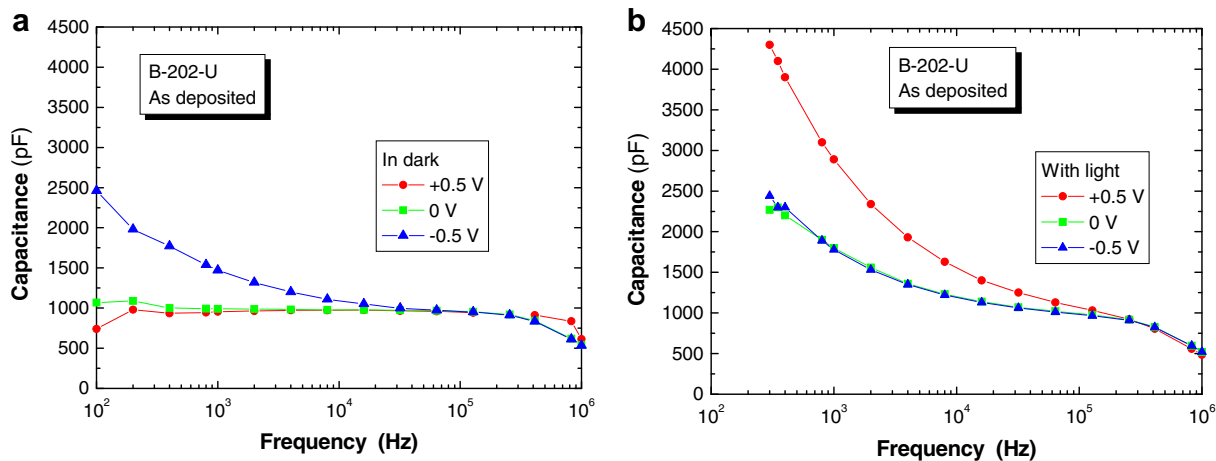


Fig. 4. Capacitance versus frequency curves, C - V - f , for different bias conditions in the as deposited detector B-201-U (a) in dark and (b) under HeNe illumination. Essential parameters are room temperature, 1 kHz modulation frequency, and 100 mV modulation voltage.

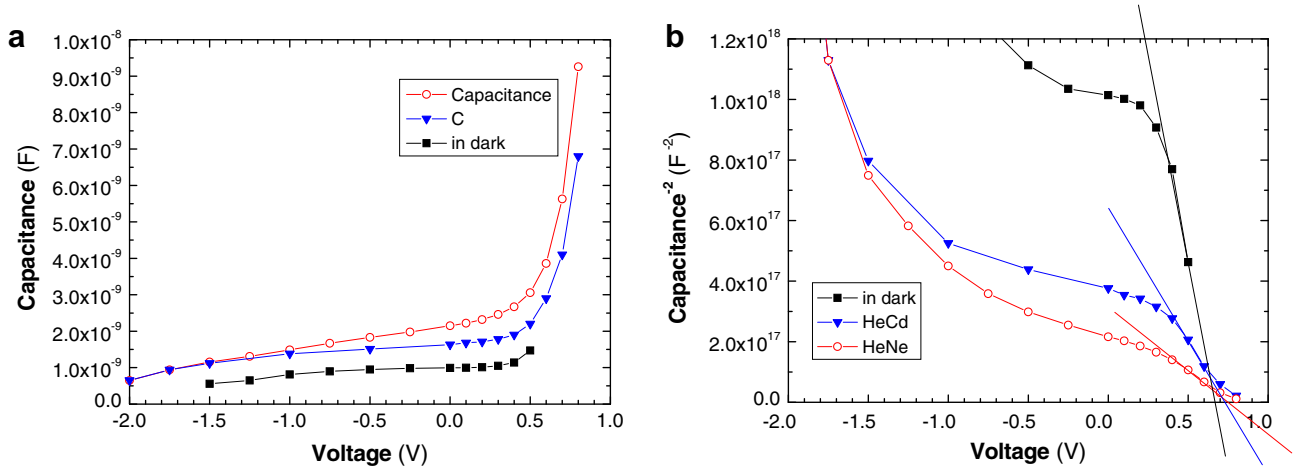


Fig. 5. (a) Dark capacitance and photocapacitance versus applied bias for HeCd (325 nm) and HeNe laser illumination (633 nm). (b) $1/C^2$ plot which hints to a built-in potential of about 0.68 eV in the dark, and 0.72 and 0.75 eV under illumination, respectively. Note that, in general, the Mott plot cannot be applied for forward bias operation.

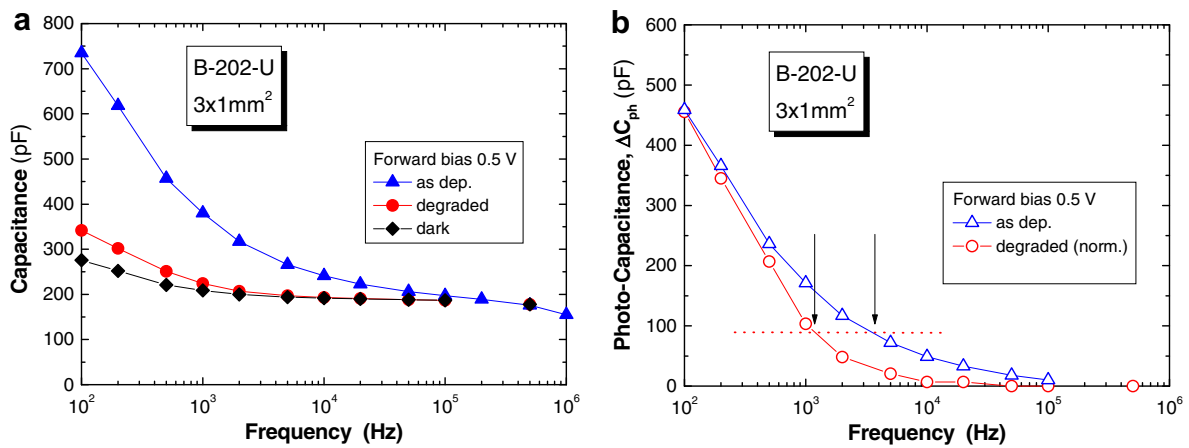


Fig. 6. (a) Photocapacitance versus frequency, $C-f$, for the as deposited detector B-201-U and after 4He^+ bombardment, in comparison with the dark capacitance. (b) Capacitance change upon illumination in both cases showing the shift of the cut-off frequency from 3.5 to 1.2 kHz after irradiation.

As far as the scan across the degraded pixel is concerned, we have taken photocurrent scans with the same modulated laser light and found a shape of the dip similar to the one shown in Fig. 3. Using two different intensity filters we found that in contrast to the photocurrent case, the photocapacitance signal increases sub-linearly with light intensity. We will need more data and comparison with numerical simulation to further quantify this particular light dependence.

The $C-V-f$ plots in the following figures all show that the photocapacitance is large under forward bias condition. This indicates a favourable region for studying defects, either intrinsic ones or irradiation induced defects. Under reverse bias we would see the transport of carriers across the sample within the time window given by the modulation frequency. In forward bias we would push the carriers towards the center of the device and favour the observation of carrier recombination.

It is surprising that the straight line tests of Fig. 5 lead actually to reasonable values of the built-in potential of about 0.68 eV in the dark, and 0.72 and 0.75 eV under illumination with HeNe and HeCd laser irradiation, respectively. On the other hand the change of wavelength from 633 nm (HeNe laser) to 325 nm (HeCd) did not affect the overall shape of the $C-V-f$ plots.

We can explain the change of the cut-off frequency in the last figure by the assumption of reduced carrier mobility after ion bombardment. This would lead to less efficient collection of the photocharge at higher frequencies.

5. Conclusion

We could show that the photocapacitance method can be applied to thin film p-i-n detector structures to study the degradation behaviour after particle bombardment. Time-resolved measurements can reveal trap levels of

charges in deep defects. It is also possible to map a degraded area by spatially-resolved phot capacitance with a resolution that is mainly limited by the scanning laser beam diameter.

Acknowledgements

The authors acknowledge financial support from the Portuguese Foundation for Science and Technology, through projects POCTI/FP/FNU/50352/2003 (MSIC-2), POCTI/CTM/41317/2001 (SICAL), and POCI/CTM/56078/2004 (LAXOR), and through the R&D unit no 631 Center of Electronics, Optoelectronics and Telecommunications (CEOT) in Faro. We are grateful to F. Wuensch and M. Kunst, HMI, and to A. Nathan, Univer-

sity of Waterloo, for supplying the samples, and to E. Alves and C.P. Marques for particle irradiation.

References

- [1] J.J. Wysocki, *IEEE Trans. Nucl. Sci.* (1963) 80.
- [2] A.V. Gelatos, J.D. Cohen, J.P. Harbison, *Appl. Phys. Lett.* 49 (1986) 772.
- [3] M. Vanacek, J. Kocka, J. Stuchlik, Z. Kozisek, O. Stika, A. Triska, *Sol. Energy Mater.* 8 (1983) 411.
- [4] A.Y. Polyakov, N.B. Smirnov, A.V. Govorkov, E.A. Kozhukhova, V.I. Vdovin, K. Ip, M.E. Overberg, Y.W. Heo, D.P. Norton, S.J. Pearton, J.M. Zavada, V.A. Dravin, *J. Appl. Phys.* 94 (2003) 2895.
- [5] R.A. Enzenroth, T. Takamiya, K.L. Barth, W.S. Sampath, *Thin Solid Films* 515 (2007) 6155.
- [6] Q. Wang, R.S. Crandall, E.A. Schiff, in: *Proceedings of the 21st Photovoltaics Specialists Conference, IEEE, 1996*, p. 1113.
- [7] I. Nurdjaja, E.A. Schiff, *Mater. Res. Soc. Symp. Proc.* 467 (1997) 723.